I&EC research
Industrial & Engineering Chemistry Research

Article

pubs.acs.org/IECR

$Ce_{0.8}Sm_{0.15}Sr_{0.05}O_2$ as Possible Oxidation Catalyst and Assessment of the CaO Addition in the Coupled CO Oxidation−CO_2 Capture Process

Oscar Ovalle-Encinia,[†] J. Arturo Mendoza-Nieto,[†] José Ortiz-Landeros,[‡] and Heriberto Pfeiffer*[,†]

[†]Laboratorio de Fisicoquímica y Reactividad de Superficies (LaFReS), Instituto de Investigaciones en Materiales, Universidad Nacional Autónoma de México, Circuito exterior s/n, Cd. Universitaria, Del. Coyoacán, CP 04510, Ciudad de México, Mexico

[‡]Departamento de Ingeniería en Metalurgia y Materiales, Escuela Superior de Ingeniería Química e Industrias Extractivas, IPN, UPALM, Av. Instituto Politécnico Nacional s/n, CP 07738, Ciudad de México, Mexico

ABSTRACT: A synergetic system for the coupled CO oxidation and CO_2 trapping was proposed and studied in the present work by using a ceria-based material and CaO as catalyst and absorbent, respectively. Specifically, $Ce_{0.8}Sm_{0.15}Sr_{0.05}O_2$ (CSSO) was synthesized by the EDTA−citrate complexing method and the resultant powders were characterized by XRD, SEM, and N_2 adsorption−desorption measurements. The structure was identified as a fluorite phase, and the BET analysis showed specific areas of 25.6 and 2.6 m^2/g for the samples heat-treated at 650 and 1000 °C, respectively. Dynamic thermogravimetric analyses performed under CO_2, CO, CO−O_2, and O_2 containing atmospheres showed the thermal stability and reactivity of the ceria-based catalyst. Then, the CO oxidation tests were evaluated in two stages: first, the dynamic and isothermal analyses for the CO oxidation by the CSSO treated at 650 and 1000 °C; then, the evaluation of the CO oxidation properties of the proposed catalyst with in situ CO_2 capture by adding CaO to the system. The results for the CSSO1000−CaO system evidenced simultaneous double process produced by the synergetic CO oxidation at temperatures between 350 and 650 °C and the CO_2 chemisorption on the CaO. Furthermore, the combined materials reduce the different temperature processes probably due to the CaO partial catalytic activity.

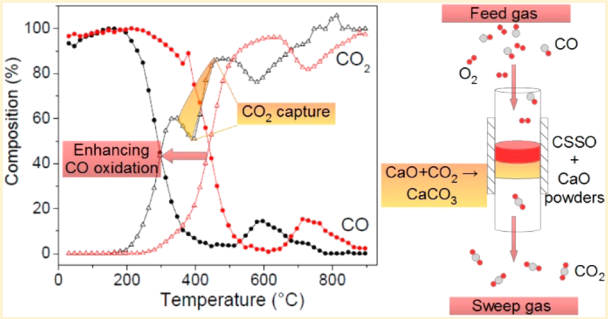

INTRODUCTION

Carbonaceous combustion products such as carbon dioxide (CO_2) and carbon monoxide (CO) are hazardous gaseous atmospheric pollutants.[1,2] CO_2 is the main greenhouse gas, reaching in 2014 a global annual emission higher than 32 Gt according to the International Energy Agency.[3] In the same sense, a million tons of CO are emitted from industrial, domestic, and transport sources due to incomplete combustion of hydrocarbons.[2] The increasing concentration of these pollutants in the atmosphere could spiral into undesirable environmental and public health issues.[4,5]

Several strategies have been proposed as a means to decrease the emissions of CO_2 into the atmosphere, for example, through the capture,[1,6−8] utilization,[9,10] or sequestration based technologies.[11−13] Regarding carbon monoxide, the CO oxidation process to CO_2 has been widely studied in the last decades, using different supported metallic catalysts.[14−17] Apart from this, CO is produced as a syngas component (H_2 + CO), e.g., during dry methane reforming.[18,19] Syngas can be used as flammable gas, or the syngas components can be separated in order to obtain hydrogen enriched gas.[20,21] The CO separation process is usually performed through an oxidation process, which facilitates the hydrogen enrichment, where noble metals on ionically conducting ceramics as active catalyst supports, such as ceria (CeO_2), have shown high CO oxidation properties.[22−24] The catalytic properties of CeO_2 are found in its ability to work in oxidizing and reducing conditions (the ability of cerium to cycle between and Ce^{4+} and Ce^{3+}), exhibiting the so-called "oxygen storage capacity".[24] Besides the intrinsic redox properties, doped CeO_2 systems have been widely studied to promote a higher ionic conduction than a single ceria.[24,25] Moreover, there are several studies showing that the presence of dopants and codopants on CeO_2 increases the formation of oxygen vacancies in the crystalline structure on which oxygen ion transport is highly associated.[25−28] For example, Zhu and co-workers recently reported that a composite based on Sm-doped CeO_2 (SDC) materials can be used for oxygen permeation membranes.[27] Moreover, a catalyst-free tubular membrane reactor based on an SDC−carbonate dual phase membrane was proposed by Lin and co-workers.[28] This reactor shifts reaction from the hot gasifier syngas to H_2 and CO_2 with simultaneous separation of CO_2.

On the other hand, recently different ceramic oxides have been proposed for CO capture,[29−31] through the CO oxidation and the subsequent chemisorption of the formed CO_2.

Received: December 16, 2016
Revised: May 3, 2017
Accepted: May 9, 2017
Published: May 9, 2017

DOI: 10.1021/acs.iecr.6b04872
Ind. Eng. Chem. Res. 2017, 56, 6124−6130

Depending on the operation temperature range, these materials have potential for the development of respiratory protection systems for evacuation and rescue in fire smoke, scavenging sorbent for postfire cleanup, simultaneous trapping of CO and CO_2 products coming from coal and biomass combustion, and CO removal to obtain H_2-rich syngas.[29−31] Among the all the high temperature CO_2 capture materials proposed in the literature, calcium oxide (CaO) possesses excellent properties, and there are several studies showing how the CO_2 capture properties can be optimized varying CaO structural and/or microstructural characteristics.[32−37]

Base on the above, the aim of the present work was divided in two different sections. (1) Investigate the ability of $Ce_{0.8}Sm_{0.15}Sr_{0.05}O_2$ as a possible catalyst for the CO oxidation process, under different microstructural conditions at intermediate temperature. (2) Evaluate the possible coupling between $Ce_{0.8}Sm_{0.15}Sr_{0.05}O_2$ and calcium oxide (CaO) material as a CO oxidant and an in situ CO_2 captor bifunctional system. In this approach, $Ce_{0.8}Sm_{0.15}Sr_{0.05}O_2$ and CaO were chosen due to the following factors. In the case of ceria, it was chosen due to its oxygen storage and diffusion capacities, which must be improved by the doping proposed, while in the case of CaO, it was chosen because of its already known CO_2 capture properties at intermediate and high temperatures.[35−37] These oxidation-capture analyses were performed dynamically and isothermally at different temperatures, varying the ceramic catalyst surface features and the calcium oxide addition as a CO_2 chemisorbent.

EXPERIMENTAL SECTION

$Ce_{0.8}Sm_{0.15}Sr_{0.05}O_2$ (CSSO) was synthesized by the EDTA−citrate complexing method in order to obtain the corresponding ceramics with the highest homogeneity and crystallinity at moderate and high temperatures. CSSO was obtained in the presence of two organic acids: citric acid anhydrous ($C_6H_8O_7$ 99.98% from Sigma-Aldrich) and ethylenediaminetetraacetic acid (EDTA, $C_{10}H_{16}N_2O_8$, 98.5% from Sigma-Aldrich).[38] Stoichiometric amounts of each metal nitrate ($Ce(NO_3)_3\cdot 6H_2O$ 99.0% from Sigma-Aldrich; $Sm(NO_3)_3\cdot 6H_2O$ 99.9% from Sigma-Aldrich; and $Sr(NO_3)_2$ 99.0% from Meyer) were fully dissolved in deionized water. Then, equimolar amounts of citric acid and EDTA were added to the nitrate solution, dissolved in ammonium hydroxide (28.0−30.0%, Baker ACS Reagent). The pH value was adjusted to 6−8, using ammonium hydroxide. A transparent solution was obtained and heated to 90 °C, while stirring. After a partial evaporation process, a white paste was obtained and heated to 300 °C, in order to remove the nitrate and organic compounds. The resultant powder was heated at 650 °C for 10 h and 1000 °C for 40 h. Samples were calcined for long times (40 h) with the aim to determine their stability as a function of temperature and time. Subsequently powders were milled using a mortar and pestle to yield homogeneous powders labeled as CSSO650 and CSSO1000, respectively.

The structural and microstructural characterization of the sample was performed using different techniques. A diffractometer (Siemens, D5000) with a Co Kα (1.7903 Å) radiation source operating at 34 kV and 30 mA was used to identify the fluorite phase and the products after the CO oxidation analyses. The samples were measured in a 2θ range of 20−80° with a step size of 0.02°. The phases were identified using the Joint Committee Powder Diffraction Standards (JCPDS). Additionally, the products after CO oxidation tests were analyzed by Fourier transform infrared (FTIR) spectroscopy using Alpha Platinum equipment from Bruker connected to a diamond attenuated total reflectance (ATR) cell. The microstructure was analyzed using scanning electron microscopy (SEM) and N_2 adsorption−desorption. The SEM analysis was performed on a JEOL JMS-7600F, while the nitrogen adsorption−desorption isotherms were obtained on a Bel-Japan Minisorp II instrument at 77 K using a multipoint technique (N_2 from Praxair, grade 4.8). Prior to analysis, samples were degassed at room temperature for 24 h. The surface areas were determined using the Brunauer−Emmett−Teller (BET) method.

Different dynamic controlled atmosphere experiments were performed to analyze the chemical reaction of the CSSO powders sintered at 1000 °C. Those experiments were made on a Q500HR thermobalance (TA Instruments). Initially, the sample was dynamically heated from 30 to 900 °C at 5 °C/min, using different gas atmospheres: (i) 60 mL·min^{-1} CO_2 (Praxair, grade 3.0), (ii) 60 mL·min^{-1} CO (5% vol in N_2 Praxair, certificate standard), (iii) 57−3 mL·min^{-1} CO−O_2, and (iv) 3 mL·min^{-1} O_2 (Praxair, grade 2.6), all diluted in N_2 to complete 100 mL·min^{-1} as a total gas flow.

The CO oxidation process, for CSSO650 and CSSO1000 catalysts, was evaluated in a catalytic reactor (Bel-Japan, Model Bel-Rea) using a gas mixture of 5−3 mL·min^{-1} CO−O_2 (a total flow rate of 100 mL·min^{-1} and 200 mg of catalyst). Initially, the samples were cleaned under 50 mL·min^{-1} N_2 for 10 min. Then, the samples were dynamically heated from 30 to 900 °C at a heating rate of 2 °C·min^{-1}, under the CO−O_2 gas mixture. For the isothermal analysis, the samples were cleaned and heated at 15 °C·min^{-1} to the corresponding temperature (between 350 and 750 °C) under a N_2 flux. Once the corresponding temperature was reached, the flow gas was switched from N_2 to the desired gas mixture during 3 h. The gas products were analyzed with a GC-2014 gas chromatograph (Shimadzu) with a Carboxen-1000 column. Additionally, a second set of CO oxidation experiments were performed using calcium oxide (CaO), which was obtained by calcining calcium carbonate ($CaCO_3$, Meyer 99.9%) at 900 °C for 6 h. CaO crystalline structure was confirmed by X-ray diffraction (XRD) and the sample was microstructurally characterized by N_2 adsorption, where the sample presented a specific surface area of 14 m^2/g (data not shown).[37] In these experiments, a CaO layer was placed in the tubular reactor over a quartz fiber; then, a second layer of CSSO1000 was placed on the CaO layer. The addition of CaO was done in order to identify if the CO_2 produced by the CSSO1000 sample could be trapped chemically in the same reactor flow. These experiments were performed using a CSSO/CaO molar ratio of 1/3, where the CaO excess was used to ensure the visualization of the CO_2 capture process. Additionally, this CSSO/CaO molar ratio corresponds to a CSSO/CaO mass ratio of 1. All these experiments were performed using the same thermal conditions, described above, for the catalytic tests.

RESULTS AND DISCUSSION

CSSO650 and CSSO1000 samples were structurally characterized by XRD and microstructurally by SEM and N_2 physisorption techniques. Figure 1 shows the XRD patterns fitted with the PDF 43-1002 file; both samples correspond to the ceria crystalline structure with space group $Fm\bar{3}m$. Certain differences in the diffraction width peaks, that reveal differences on the crystal size of the samples. In fact, crystal size was evidently reduced, from 146 nm to about 14 nm in the

DOI: 10.1021/acs.iecr.6b04872
Ind. Eng. Chem. Res. 2017, 56, 6124−6130

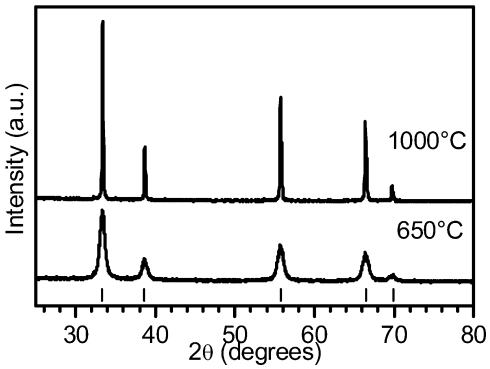

Figure 1. X-ray diffraction patterns for CSSO materials heat-treated at 650 and 1000 °C. At the bottom, the vertical marks correspond to the ceria Bragg reflections (PDF 43-1002).

CSSO1000 and CSSO650 samples, respectively. No other crystalline phases were detected, at least at the XRD detection level.

The same as before, the microstructural characterization of the samples clearly showed changes in comparison. In the case of the sample CSSO650, SEM images showed the formation of tiny polyhedral particles smaller than 20 nm (Figure 2A). This

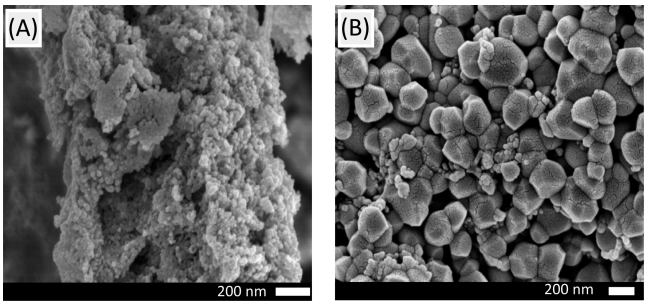

Figure 2. SEM images for CSSO materials heat-treated at 650 (A) and 1000 °C (B).

means an important smaller size in comparison to the CSSO1000 case, where the particle size was around 150−200 nm (Figure 2B). These changes must be attributed to the synthesis temperature. As in the SEM analysis, the N_2 adsorption results showed some marked variations (Figure 3). The CSSO1000 sample presented an isotherm type II without hysteresis, according with the IUPAC classification;[39] this kind of curve is presented for nonporous materials. In the CSSO650 sample, it presented the same isotherm type II but with a

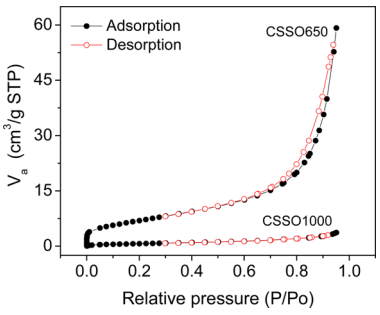

Figure 3. Nitrogen adsorption−desorption isotherms for CSSO materials heat-treated at 650 and 1000 °C.

narrow hysteresis loop, indicating the presence of some mesoporosity (pore diameter of 14.2 nm and pore volume of 0.0915 cm^3/g). Additionally, the BET surface area varied almost 10 times between CSSO650 and CSSO1000 samples (25.6 and 2.6 m^2/g, respectively), which must be related to the lower particle size and mesoporosity observed in the CSSO650 sample. Moreover, all these results are in good agreement with the final temperature used during synthesis (650 and 1000 °C).

After microstructural characterization, the thermal stability of samples was evaluated by thermogravimetric (TG) experiments, performing dynamic TG under four different atmospheres (CO_2, O_2, CO, and CO + O_2). These results are presented in Figure 4. Results were similar in both cases, and

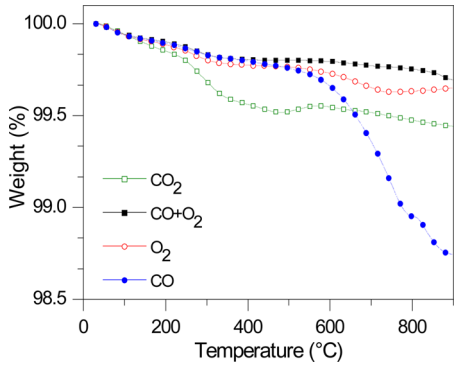

Figure 4. Dynamic thermograms for CSSO1000 sample treated under different atmospheres, all diluted in N_2 to complete 100 mL/min as a total gas flow.

only thermograms for CSSO1000 material are shown. The sample did not present important weight changes (≤0.5 wt %) when it was thermally treated under CO_2 (which indicated a negligible possible carbonation process) or oxidative atmospheres (O_2 and CO + O_2). However, when only CO was used, a reductive atmosphere, the sample presented a weight decrease of 1.3 wt % between 500 and 900 °C. In this case, the weight decrement may be associated with a partial superficial reduction, through the superficial oxygen release that is tentatively consumed by the CO oxidation. In any case, when CO was added with O_2, the superficial reduction was not observed due to the oxygen partial pressure in the system, which maintains the lattice oxygen stoichiometry of the compound. These results were confirmed and were consistent with results obtained after the CO oxidation study (see results below).

In order to analyze the materials capacity for the CO oxidation process; the catalyst samples were dynamically evaluated in a catalytic reactor connected to a gas chromatograph (Figure 5). It can be seen that the CSSO650 catalyst shows a slightly higher catalytic activity at lower temperatures than the CSSO1000 catalyst. In the first case, a 100% CO conversion was reached at 500 °C, while that for CSSO1000 was reached around 540 °C. Thus, the heat treatment and the resulted microstructural features of the samples have an effect on the catalyst activity for low and intermediate temperature CO oxidation. It should be mentioned that CO conversion performed on the CSSO1000 sample presented a higher fluctuation, or partial instability, than the CSSO650 sample, although both samples presented a similar thermal trend. It should be associated with the microstructural variations of both samples, described above. In any case, and in order to evaluate

DOI: 10.1021/acs.iecr.6b04872
Ind. Eng. Chem. Res. 2017, 56, 6124−6130

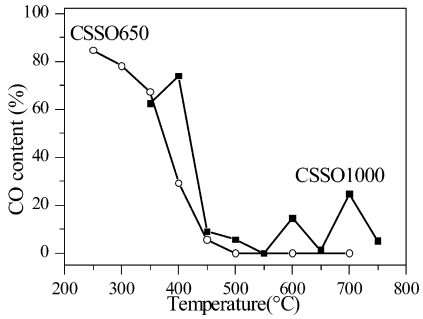

Figure 5. Carbon monoxide conversion obtained with CSSO samples.

the possible coupling between $Ce_{0.8}Sm_{0.15}Sr_{0.05}O_2$ and an absorbent material for the CO oxidation and in situ CO_2 capture, the sample CSSO1000 was selected because its operational temperature range matches with the selected CaO for CO_2 trapping.

Figure 6 shows a more detailed analysis of the CO catalytic transformation on the CSSO1000 sample which presented

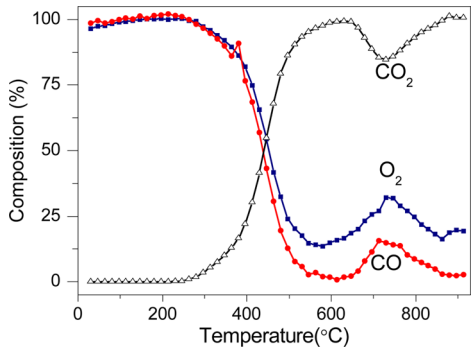

Figure 6. Dynamic evolution of reactants (CO and O_2) and product (CO_2) obtained with CSSO1000 material.

specific temperature dependence. At $T \leq 240$ °C, CO and O_2 did not appear to vary. In other words, the catalytic reaction did not occur. Nevertheless, reactant conversion (CO and O_2) to CO_2 product was observed from 250 to 900 °C, reaching a total CO conversion around 600 °C. It must be pointed out that between 650 and 870 °C the catalytic conversion decreased partially. This effect may have been produced due to changes in the sorption−desorption equilibrium.

Based on the previous dynamic behavior, different isothermal experiments were performed. Figure 7 shows that all the

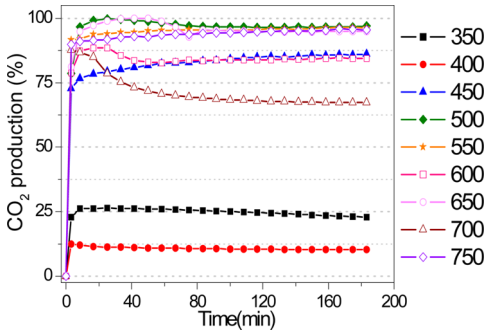

Figure 7. CO_2 formation on CSSO1000 sample during CO oxidation isotherms performed at different temperatures between 350 and 750 °C.

isotherms present an exponential behavior and the maximum amount of produced CO_2 was reached in less than 10 min of reaction time. The initial isothermal experiments were performed at 350 °C. These isotherms presented poor CO conversion efficiencies (<30%). However, at higher temperatures the CO conversion increased importantly to 70%, or higher efficiencies. In fact, as in the dynamic analysis, these isotherms showed the highest CO catalytic conversion between 500 and 650 °C. Once again, it is remarkable that the CO conversion to CO_2 is produced in the same temperature range where the CO_2 is trapped by different alkaline and earth alkaline ceramics including CaO.[1,29,30,36]

After the CO oxidation experiments, all the isothermal products were characterized in order to identify any possible structural modification or reaction due to gas chemisorption. Figures 8 and 9 show the XRD patterns and ATR-FTIR spectra

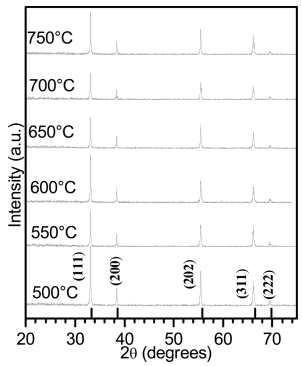

Figure 8. X-ray patterns of CSSO1000 products obtained after CO oxidation isotherms performed between 500 and 750 °C. At the bottom, the vertical marks correspond to the ceria Bragg reflections (PDF 43-1002).

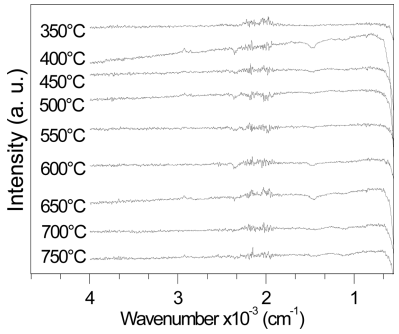

Figure 9. ATR-FTIR spectra for CSSO1000 products obtained after CO oxidation isotherms performed between 350 and 750 °C.

of the CSSO1000 samples, respectively, after each isothermal experiment. From these characterization techniques, it can be seen that there were no structural changes (Figure 8, XRD pattern) or the presence of reaction products due to gas chemisorption (Figure 9, ATR-FTIR). These results confirmed the high CSSO1000 thermal and chemical stability under these physicochemical conditions.

After the CO oxidation test on both CSSO samples, CaO was used as a possible CO_2 captor into the same reaction system, in order to evaluate the CO oxidation and subsequent CO_2 capture. CSSO1000 sample was used, because the temperature range where CO_2 was produced with this sample, between 650 and 800 °C, matched with the CO_2 capture

DOI: 10.1021/acs.iecr.6b04872
Ind. Eng. Chem. Res. 2017, 56, 6124−6130

temperature range of CaO. Thus, the CSSO1000 sample should not present any change due to its thermal history evolution. Figure 10 shows the dynamic CO and CO_2 evolution

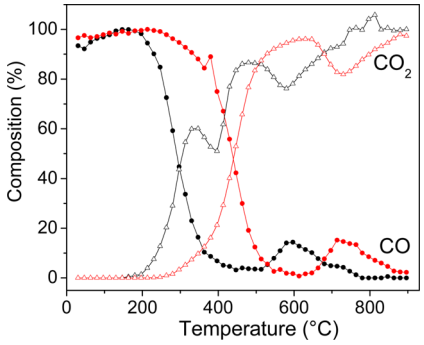

Figure 10. Dynamic evolution of CO and CO_2 using CSSO1000 material (red lines) and CSSO1000−CaO system (black lines).

as a function of temperature for the CSSO1000−CaO layer arrangement and the CSSO1000 sample for comparison purposes. As can be seen, although the gas evolution, determined by the gases released from the catalytic reactor, was similar in both cases, the CaO addition induced some specific and interesting changes. Initially, the general process was shifted to lower temperatures around 200 °C. With the presence of CaO the CO oxidation process began at approximately 200 °C; 100% CO conversion was observed at 430 °C. Also, the CO conversion decrement observed between 650 and 870 °C for the CSSO1000 sample was shifted to lower temperatures.

By contrast, the CO_2 production presented the same general behavior observed for CO, with the corresponding temperature shifts. However, the CO_2 formation evolution seemed to be lower than with CO, and it presented two specific decrements around 400 and 580 °C. These variations must be associated with the CO_2 capture produced over the surface and bulk of CaO, reducing the CO_2 concentration at the sweep gas. In fact, similar results have been reported for other CaO systems, where the CO oxidation and subsequent CO_2 chemisorption have been analyzed.[37]

Therefore, these results evidenced the double process produced by the CSSO1000−CaO system: the CO oxidation and CO_2 chemisorption (capture). Furthermore, the CSSO1000−CaO system reduced the process temperature, which may be related to the CaO partial catalytic activity reported previously for the CO oxidation reaction.[37] Between 780 and 830 °C, a higher amount of CO_2 than 100% was detected by GC. According to a previous work,[37] this behavior can be associated with the CO_2 desorption process that takes place at these temperatures in the CaO material.

In order to further analyze the CO oxidation by the CSSO1000−CaO system, different isothermal analyses were performed from 350 to 700 °C (Figure 11A). The CSSO1000−CaO isotherms presented trends similar to those previously obtained in the case of CaO absence (Figure 7). For all the isotherms the maximum amount of CO_2 was obtained after 20 min of reaction time, except for the isotherm performed at the lowest temperature (350 °C), where the maximum amount of CO_2 was detected after almost 80 min. These average times were larger than those obtained in the case of CaO absence. Thus, these results confirm the fact that CaO is capturing part of the CO_2 produced by the CSSO1000 catalyst, retarding the

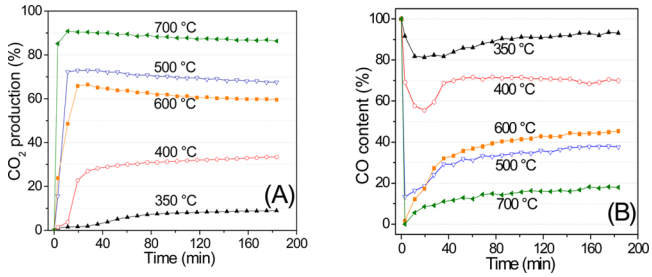

Figure 11. CO_2 formation (A) and CO conversion (B) during CO oxidation isotherms performed between 350 and 700 °C, using the CSSO1000−CaO system.

presence of CO_2 in the sweep gas mixture. The initial isothermal experiments were performed at 350 and 400 °C. In this temperature range, isotherms presented higher CO conversion efficiencies (40% at 400 °C) than in the case of CaO absence, which may be associated with the synergetic catalytic activity. Then, between 500 and 600 °C the CO_2 production was lower in the presence of CaO than in the absence of CaO; also, these isotherms showed some CO_2 production decrements as a function of the time. All these results must be associated with the fact that part of the CO_2 is been chemically trapped by CaO. Finally, at 700 °C, the CO_2 production was increased again until CO_2 production reached 91% at 11 min of reaction time, due to the combination of the CO oxidation and the $CaCO_3$ decomposition processes. Figure 11B shows the CO conversion efficiencies obtained in the same CSSO1000−CaO isothermal experiments. As could be expected, during the first reaction times all the isotherms presented the highest conversion: 19, 44, 87, and 100% at 350, 400, 500, and 600−700 °C, respectively. After that, all the isotherms presented slight CO conversion decrements, tending to similar equilibriums than those reported above for the CSSO1000 sample. Then, at the beginning of the reaction process both compounds (CSSO1000 and CaO) must participate in the CO oxidation, but as soon as CaO is carbonated, it does not contribute to the CO oxidation as can be seen during the first 30−40 min of reaction at any temperature. These results confirmed that CO conversion continues independently of the CO_2 chemisorption process performed by CaO.

CONCLUSIONS

$Ce_{0.8}Sm_{0.15}Sr_{0.05}O_2$ (CSSO) was synthesized to evaluate its possible application as carbon monoxide oxidation catalyst; additionally, the CSSO1000−CaO layer arrangement system was analyzed to determine the possible CO conversion and subsequent CO_2 chemisorption processes. Results showed that CSSO is a thermal stable ceria-based material and it can catalyze the CO oxidation reaction at temperatures equal to or higher than 300 °C, reaching 100% CO conversion between 450 and 650 °C depending on the microstructural features of the catalyst. Moreover, the addition of CaO improves the catalytic effect and allows the CO_2 chemisorption in the CSSO1000−CaO composite in a lower temperature range, without decreasing the CO oxidation capacity. All these results show the possible application of this or similar systems in the bifunctional CO oxidation and in situ CO_2 capture processes, which may be useful in different industrial applications where CO must be separated from certain gaseous effluents such as

DOI: 10.1021/acs.iecr.6b04872
Ind. Eng. Chem. Res. 2017, 56, 6124−6130

flue gas or the separation of carbon monoxide present as a syngas component.

AUTHOR INFORMATION

Corresponding Author

*Tel.: +52 (55) 5622 4627. E-mail: pfeiffer@iim.unam.mx.

ORCID

Heriberto Pfeiffer: 0000-0002-6217-3420

Notes

The authors declare no competing financial interest.

ACKNOWLEDGMENTS

O.O.-E. and J.A.M.-N. thank CONACYT and DGAPA-UNAM, respectively, for financial support. Moreover, this work was financially supported by SENER-CONACYT (251801).

REFERENCES

(1) Lee, S.-Y.; Park, S.-J. A Review on Solid Adsorbents for Carbon Dioxide Capture. *J. Ind. Eng. Chem.* **2015**, *23*, 1.

(2) Chen, R.; Pan, G.; Zhang, Y.; Xu, Q.; Zeng, G.; Xu, X.; Chen, B.; Kan, H. Ambient Carbon Monoxide and Daily Mortality in Three Chinese Cities: The China Air Pollution and Health Effects Study (CAPES). *Sci. Total Environ.* **2011**, *409*, 4923.

(3) *CO_2 Emissions from Fuel Combustion Highlights*; International Energy Agency: 2016.

(4) Prasad, P. V. V.; Thomas, J. M. G.; Narayanan, S. Global Warming Effects. In *Encyclopedia of Applied Plant Sciences*; Elsevier: 2017; pp 289−299.

(5) Chen, T.-M.; Kuschner, W. G.; Gokhale, J.; Shofer, S. Outdoor Air Pollution: Nitrogen Dioxide, Sulfur Dioxide, and Carbon Monoxide Health Effects. *Am. J. Med. Sci.* **2007**, *333*, 249.

(6) Wang, S.; Yan, S.; Ma, X.; Gong, J. Recent Advances in Capture of Carbon Dioxide Using Alkali-Metal-Based Oxides. *Energy Environ. Sci.* **2011**, *4*, 3805.

(7) Mendoza-Nieto, J. A.; Pfeiffer, H. Thermogravimetric Study of Sequential Carbonation and Decarbonation Processes over Na_2ZrO_3 at Low Temperatures (30−80 °C): Relative Humidity Effect. *RSC Adv.* **2016**, *6*, 66579.

(8) Díaz-Herrera, P. R.; Ramírez-Moreno, M. J.; Pfeiffer, H. The Effects of High-Pressure on the Chemisorption Process of CO_2 on Lithium Oxosilicate (Li_8SiO_6). *Chem. Eng. J.* **2015**, *264*, 10.

(9) Galvita, V. V.; Poelman, H.; Bliznuk, V.; Detavernier, C.; Marin, G. B. CeO_2 -Modified Fe_2O_3 for CO_2 Utilization via Chemical Looping. *Ind. Eng. Chem. Res.* **2013**, *52*, 8416.

(10) Ampelli, C.; Perathoner, S.; Centi, G. CO_2 Utilization: An Enabling Element to Move to a Resource- and Energy-Efficient Chemical and Fuel Production. *Philos. Trans. R. Soc., A* **2015**, *373*, 20140177.

(11) Miller, B. Greenhouse Gas − Carbon Dioxide Emissions Reduction Technologies. In *Fossil Fuel Emissions Control Technologies*; Elsevier: 2015; pp 367−438.

(12) Mondal, M. K.; Balsora, H. K.; Varshney, P. Progress and Trends in CO_2 Capture/separation Technologies: A Review. *Energy* **2012**, *46*, 431.

(13) Figueroa, J. D.; Fout, T.; Plasynski, S.; McIlvried, H.; Srivastava, R. D. Advances in CO_2 Capture technology—The U.S. Department of Energy's Carbon Sequestration Program. *Int. J. Greenhouse Gas Control* **2008**, *2*, 9.

(14) Anil, C.; Madras, G. Kinetics of CO Oxidation over Cu Doped Mn_3O_4. *J. Mol. Catal. A: Chem.* **2016**, *424*, 106.

(15) Haneda, M.; Todo, M.; Nakamura, Y.; Hattori, M. Effect of Pd Dispersion on the Catalytic Activity of Pd/Al_2O_3 for C_3H_6 and CO Oxidation. *Catal. Today* **2017**, *281*, 447.

(16) Sandoval, A.; Zanella, R.; Klimova, T. E. Titania Nanotubes Decorated with Anatase Nanocrystals as Support for Active and Stable Gold Catalysts for CO Oxidation. *Catal. Today* **2017**, *282*, 140.

(17) Sandoval, A.; Aguilar, A.; Louis, C.; Traverse, A.; Zanella, R. Bimetallic Au−Ag/TiO_2 Catalyst Prepared by Deposition−precipitation: High Activity and Stability in CO Oxidation. *J. Catal.* **2011**, *281*, 40.

(18) Laosiripojana, N.; Assabumrungrat, S. Catalytic Dry Reforming of Methane over High Surface Area Ceria. *Appl. Catal., B* **2005**, *60*, 107.

(19) Mendoza-Nieto, J. A.; Vera, E.; Pfeiffer, H. Methane Reforming Process by Means of a Carbonated-Na_2ZrO_3 Catalyst. *Chem. Lett.* **2016**, *45*, 685.

(20) Avgouropoulos, G.; Ioannides, T. Selective CO Oxidation over CuO-CeO_2 Catalysts Prepared via the Urea−nitrate Combustion Method. *Appl. Catal., A* **2003**, *244*, 155.

(21) Li, H.; Yu, K.; Wan, C.; Zhu, J.; Li, X.; Tong, S.; Zhao, Y. Comparison of the Nickel Addition Patterns on the Catalytic Performances of $LaCoO_3$ for Low-Temperature CO Oxidation. *Catal. Today* **2017**, *281*, 534.

(22) Sun, S.; Mao, D.; Yu, J. Enhanced CO Oxidation Activity of CuO/CeO_2 Catalyst Prepared by Surfactant-Assisted Impregnation Method. *J. Rare Earths* **2015**, *33*, 1268.

(23) Rida, K.; López Cámara, A.; Peña, M. A.; Bolívar-Díaz, C. L.; Martínez-Arias, A. Bimetallic Co−Fe and Co−Cr Oxide Systems Supported on CeO_2: Characterization and CO Oxidation Catalytic Behaviour. *Int. J. Hydrogen Energy* **2015**, *40*, 11267.

(24) Vernoux, P.; Lizarraga, L.; Tsampas, M. N.; Sapountzi, F. M.; De Lucas-Consuegra, A.; Valverde, J.-L.; Souentie, S.; Vayenas, C. G.; Tsiplakides, D.; Balomenou, S.; Baranova, E. A. Ionically Conducting Ceramics as Active Catalyst Supports. *Chem. Rev.* **2013**, *113*, 8192.

(25) Montini, T.; Melchionna, M.; Monai, M.; Fornasiero, P. Fundamentals and Catalytic Applications of CeO_2 -Based Materials. *Chem. Rev.* **2016**, *116*, 5987.

(26) Mukherjee, D.; Rao, B. G.; Reddy, B. M. CO and Soot Oxidation Activity of Doped Ceria: Influence of Dopants. *Appl. Catal., B* **2016**, *197*, 105.

(27) Zhu, X.; Liu, Y.; Cong, Y.; Yang, W. $Ce_{0.85}Sm_{0.15}O_{1.925}$−$Sm_{0.6}Sr_{0.4}Al_{0.3}Fe_{0.7}O_3$ Dual-Phase Membranes: One-Pot Synthesis and Stability in a CO_2 Atmosphere. *Solid State Ionics* **2013**, *253*, 57.

(28) Dong, X.; Lin, Y. Catalyst-Free Ceramic-Carbonate Dual Phase Membrane Reactor for Hydrogen Production from Gasifier Syngas. *J. Membr. Sci.* **2016**, *520*, 907.

(29) Vera, E.; Alcántar-Vázquez, B.; Pfeiffer, H. CO_2 Chemisorption and Evidence of the CO Oxidation−chemisorption Mechanisms on Sodium Cobaltate. *Chem. Eng. J.* **2015**, *271*, 106.

(30) Alcántar-Vázquez, B.; Duan, Y.; Pfeiffer, H. CO Oxidation and Subsequent CO_2 Chemisorption on Alkaline Zirconates: Li_2ZrO_3 and Na_2ZrO_3. *Ind. Eng. Chem. Res.* **2016**, *55*, 9880.

(31) Guo, Y.; Zhao, C.; Li, C.; Lu, S. Low-Temperature CO Catalytic Oxidation over KOH-Hopcalite Mixtures and In Situ CO_2 Capture from Fire Smoke. In *Fire Science and Technology 2015*; Springer Singapore: Singapore, 2017; pp 725−733.

(32) Akgsornpeak, A.; Witoon, T.; Mungcharoen, T.; Limtrakul, J. Development of Synthetic CaO Sorbents via CTAB-Assisted Sol-Gel Method for CO_2 Capture at high Temperature. *Chem. Eng. J.* **2014**, *237*, 189.

(33) Witoon, T. Characterization of Calcium Oxide Derived from Waste Eggshell and its Application as CO_2 Sorbent. *Ceram. Int.* **2011**, *37*, 3291.

(34) Witoon, T.; Mungcharoen, T.; Limtrakul, J. Biotemplated Synthesis of Highly Stable Calcium-Based Sorbents for CO_2 Capture via a Precipitation Method. *Appl. Energy* **2014**, *118*, 32.

(35) Abanades, J. C.; Alonso, M.; Rodriguez, N. Experimental Validation of in Situ CO_2 Capture with CaO during the Low Temperature Combustion of Biomass in a Fluidized Bed Reactor. *Int. J. Greenhouse Gas Control* **2011**, *5*, 512.

(36) Li, Y.-J.; Zhao, C.-S.; Qu, C.-R.; Duan, L.-B.; Li, Q.-Z.; Liang, C. CO_2 Capture Using CaO Modified with Ethanol/Water Solution during Cyclic Calcination/Carbonation. *Chem. Eng. Technol.* **2008**, *31*, 237.

DOI: 10.1021/acs.iecr.6b04872
Ind. Eng. Chem. Res. 2017, 56, 6124−6130

(37) Cruz-Hernández, A.; Alcántar-Vázquez, B.; Arenas, J.; Pfeiffer, H. Structural and Microstructural Analysis of Different CaO−NiO Composites and Their Application as CO_2 or CO−O_2 Captors. *React. Kinet., Mech. Catal.* **2016**, *119*, 445.
(38) Danks, A. E.; Hall, S. R.; Schnepp, Z. The Evolution of "sol−gel" Chemistry as a Technique for Materials Synthesis. *Mater. Horiz.* **2016**, *3*, 91.
(39) Sing, K. S. W.; Everett, D. H.; Haul, R. A. W.; Moscou, L.; Pierotti, R. A.; Rouquerol, J.; Siemieniewska, T. Reporting Physisorption Data for Gas/Solid Systems. In *Handbook of Heterogeneous Catalysis*; Wiley-VCH Verlag GmbH & Co. KGaA: Weinheim, Germany, 2008.

DOI: 10.1021/acs.iecr.6b04872
Ind. Eng. Chem. Res. 2017, 56, 6124−6130